

GSA Data Repository 2015015

Supplemental Information for:

Coral macrobioerosion is accelerated by ocean acidification and nutrients

T.M. DeCarlo, A.L. Cohen, H.C. Barkley, Q. Cobban, C. Young, K.E. Shamberger, R.E. Brainard, and Y. Golbuu

Details of Carbonate System Chemistry Measurements

Mean Ω_{Arag} in the Gulf of Panama was calculated previously from in situ seawater samples collected during the day and night during one wet and one dry season (Manzello et al., 2008; Manzello 2010). Seawater samples from the following sites were analyzed for both alkalinity/DIC and dissolved inorganic nutrients. On Jarvis, Kingman and Palmyra, seawater samples were collected over the course of the day (9 AM to 5 PM), over multiple years (2006, 2008, 2010), primarily in springtime (March-May). Our Jarvis data include additional Fall samples (September, 2012). To assess the representativeness of our samples of average conditions, we compared pH calculated from alkalinity and DIC analyses with pH data reported by Price et al. (2012), who deployed automated, in situ SeaFet pH sensors on the same reefs over diurnal and seasonal cycles (Table DR1). Our values are within error of the Price et al. (2012) values for each reef.

On Rose Atoll, seawater samples were collected in springtime of 2006, 2008, 2010, and 2012. Mean Ω_{Arag} (4.10) calculated from in situ alkalinity and DIC is consistent with the climatology (4.19) calculated from GLODAP/World Ocean Atlas. 6 out of 103 cores were collected from Rose Atoll and Wake Atoll. Any uncertainty in our average Ω_{Arag} estimate has a small influence on our statistical model, and our significance tests and our conclusions would remain the same if data from Rose Atoll and Wake Atoll were excluded.

Within Palau, Ω_{Arag} at each sampling site was calculated from alkalinity/DIC analyses of seawater samples collected from 6 AM to 6 PM over multiple tidal cycles, seasons and years. These data are reported in Shamberger et al., (2014). To assess the representativeness of our daytime samples of the average diurnal Ω_{Arag} , we compared our Palau Ω_{Arag} values with data recently generated from seawater samples collected every two hours for 4 consecutive days in November 2013 on both a low-pH reef and a barrier (ambient pH) reef. Daytime Ω_{Arag} was not significantly different from nighttime Ω_{Arag} over this sampling period (Table DR2; K.E. Shamberger 2014 unpublished data), and our values are within error. This suggests that sampling from dawn to dusk does not bias our estimates of the mean Ω_{Arag} of our Palau sample sites.

Computerized Tomography (CT) Scans

A Siemens Volume Zoom Spiral computerized tomography (CT) scanner at Woods Hole Oceanographic Institution was used to image the cores following the methods described in Saenger et al. (2009), Cantin et al. (2010), Vásquez-Bedoya et al. (2012), and Crook et al. (2013). The standard curve used to convert CT scan x-ray attenuation to density was constructed from nine, 3-cm diameter, dried *Porites* cores (Fig. DR1). Absolute bulk skeletal density of each standard, ranging from 0.809-1.537 g cm⁻³, was calculated as the quotient of measured core mass and volume.

Automated Analysis of CT Scan Data to Quantify Coral Skeletal Parameters (Extension, Density, Calcification)

Calcification rate (g cm⁻² yr⁻¹) was calculated as the product of extension of the coral colony surface during one year (cm yr⁻¹) and density of skeleton over the year's extension (g cm⁻³) (Barnes and Lough 1993).

Corallites were identified in each image by finding local density minima, which are the porous centers of calices surrounded by dense thecal walls. Images were first filtered with a 2-dimensional Gaussian filter (standard deviation 0.29 mm and clipped at 0.97 mm), which resulted in one local density minima per corallite (Fig. DR2). A Euclidian-distance nearest neighbors approach was used to assign each voxel within the core to the nearest corallite. The mean density of all voxels in one image assigned to a given corallite was taken as the corallite density in that image. Finding the corallite in one image nearest to the location of a corallite in the previous image connected the corallites throughout the core.

Annual density bands were identified by visual inspection of slabs digitally cut along the vertical growth axis of the cores (Fig. DR2). Local density minima (annual bands) were identified in several locations in each slab and repeated in 4 slabs throughout the core. Low-density bands were mapped in 3-dimensions by interpolating between the coordinates where the bands were marked.

Corallite density tracks were used to objectively define the locations of annual density bands. For each identified band, all corallites passing through the band were searched for local density minima within 1 mm of the identified band location. If a density minimum was found, the annual band at the location of the given corallite was shifted to match the density minimum. After making adjustments for all corallites passing through a band, the new coordinates of the band were interpolated to map the band in 3-dimensions. Bands were smoothed by a 2-dimensional Gaussian filter (standard deviation 0.97 mm and clipped at 0.97 mm).

For each year's growth (region between 2 low-density bands), all corallites were identified that extended in the core throughout the full year. A vector was fit to the 3-dimensional coordinates every 2 mm of vertical growth with the origin set to the first corallite coordinate, the vector direction determined by singular value decomposition and

the magnitude (length) determined by Euclidian distance. The sum of lengths of all vectors fit on a corallite's path between annual bands was taken as the annual extension rate of that corallite. Calcification rate was determined for each corallite as the product of annual extension and density, and all corallite calcification rates were averaged to determine the annual whole-core calcification rate. All image analyses were conducted with MATLAB 2012a.

REFERENCES CITED

- Barnes, D., and Lough, J., 1993, On the nature and causes of density banding in massive coral skeletons: *Journal of experimental marine biology and ecology*, v. 167, no. 1, p. 91-108, doi:10.1016/0022-0981(93)90186-R.
- Cantin, N.E., Cohen, A.L., Karnauskas, K.B., Tarrant, A.M., and McCorkle, D.C., 2010, Ocean warming slows coral growth in the central Red Sea: *Science*, v. 329, no. 5989, p. 322-325, doi:10.1126/science.1190182.
- Crook, E.D., Cohen, A.L., Rebolledo-Vieyra, M., Hernandez, L., and Paytan, A., 2013, Reduced calcification and lack of acclimatization by coral colonies growing in areas of persistent natural acidification: *Proceedings of the National Academy of Sciences of the United States of America*, v. 110, no. 27, p. 11044–11049, doi:10.1073/pnas.1301589110.
- Manzello, D. P., 2010, Ocean acidification hot spots: Spatiotemporal dynamics of the seawater CO₂ system of eastern Pacific coral reefs: *Limnology and Oceanography*, v. 55, no. 1, p. 239-248, doi:10.4319/lo.2010.55.1.0239.
- Manzello, D.P., Kleypas, J.A., Budd, D.A., Eakin, C.M., Glynn, P.W., and Langdon, C., 2008, Poorly cemented coral reefs of the eastern tropical Pacific: Possible insights into reef development in a high-CO₂ world: *Proceedings of the National Academy of Sciences of the United States of America*, v. 105, no. 30, p. 10450–10455, doi:10.1073/pnas.0712167105.
- Price, N. N., Martz, T. R., Brainard, R. E., and Smith, J. E., 2012, Diel variability in seawater pH relates to calcification and benthic community structure on coral reefs: *PLoS One*, v. 7, no. 8, p. e43843, doi:10.1371/journal.pone.0043843.
- Saenger, C., Cohen, A. L., Oppo, D. W., Halley, R. B., and Carilli, J. E., 2009, Surface-temperature trends and variability in the low-latitude North Atlantic since 1552: *Nature Geoscience*, v. 2, no. 7, p. 492-495, doi:10.1038/ngeo552.
- Shamberger, K.E., Cohen, A.L., Golbuu, Y., McCorkle, D.C., Lentz, S.J., and Barkley, H.C., 2014, Diverse coral communities in naturally acidified waters of a Western Pacific reef: *Geophysical Research Letters*, v. 41, no. 2, p. 499–504, doi:10.1002/2013GL058489.
- Vásquez-Bedoya, L. F., Cohen, A. L., Oppo, D. W., and Blanchon, P., 2012, Corals record persistent multidecadal SST variability in the Atlantic Warm Pool since 1775 AD: *Paleoceanography*, v. 27, no. 3, p. PA3231, doi:10.1029/2012PA002313.

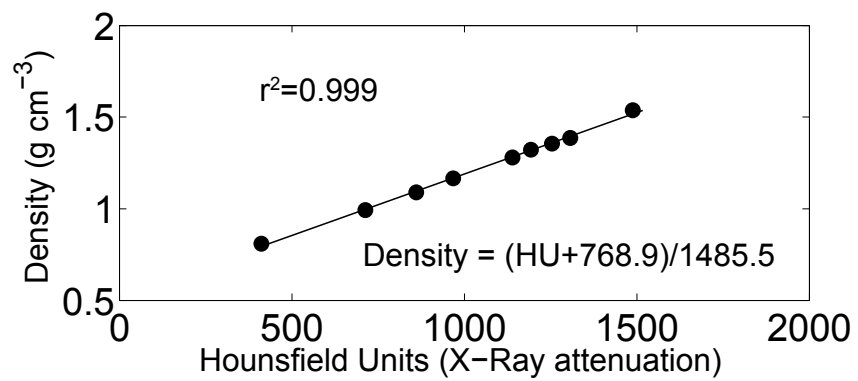


Figure DR1. Standard curve used to convert CT attenuation (Hounsfield Units) to bulk coral skeletal density (g cm⁻³).

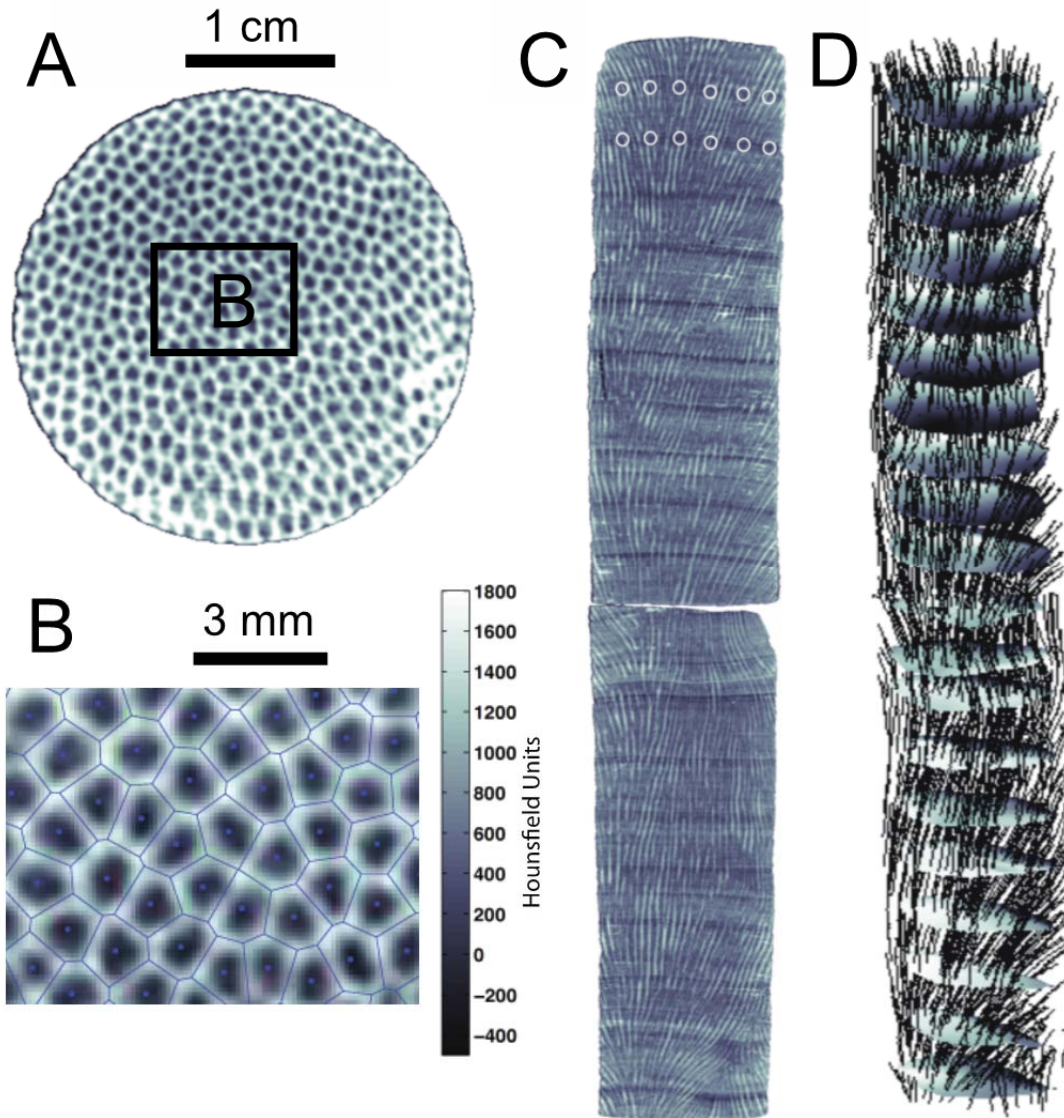


Figure DR2. Calcification rate analysis of a CT scan of a *Porites* core. A: Axial cross-section of the core that shows corallites (dark regions, low density) surrounded by skeletal walls (white, high density). B: Blue dots indicate corallites that are identified by local density minima. Blue lines show a Voronoi diagram drawn around the corallites. C: Digital slab cut in the sagittal plane. Near-vertical light and dark streaks are paths of individual corallites through the core. Horizontal dark (low density) bands are annual growth bands. The first two low-density bands are identified in the figure, as indicated by the white circles. D: 3-dimensional reconstruction of annual banding and corallite paths. Horizontal surfaces are the mapped and interpolated annual low-density bands, which are shaded to aid visualization of 3-dimensional shape. Black lines indicate paths of individual corallites traced through the core. For clarity, the image is viewed from an oblique angle looking slightly downward, and only 20% of all corallite paths are plotted. Scale bar is 1 cm and the core is 30 cm in height.

TABLE DR1. PH MEASURED ON CENTRAL PACIFIC REEFS

Reef Site	Our pH	Price et al. (2012) pH
Jarvis Island	7.98 ± 0.02	8.005 ± 0.013
Palmyra Atoll S forereef	8.007 ± 0.011	7.995 ± 0.012
Kingman Reef	8.004 ± 0.012	8.025 ± 0.009

TABLE DR2. DIURNAL VARIABILITY OF ARAGONITE SATURATION STATE (Ω) IN PALAU

Reef Site	Daytime $\Omega \pm 1\sigma$	Nighttime $\Omega \pm 1\sigma$	Average Diurnal $\Omega \pm 1\sigma$
Low pH bay reef	2.77 ± 0.05	2.74 ± 0.20	2.75 ± 0.22
Barrier reef	3.72 ± 0.27	3.57 ± 0.27	3.66 ± 0.28